





Insights into pathogenesis of fatal COVID-19 pneumonia from histopathology with immunohistochemical and viral RNA studies

Jennifer L Sauter,^{1,*}  Marina K Baine,^{1,*} Kelly J Butnor,² Darren J Buonocore,¹ Jason C Chang,¹ Achim A Jungbluth,¹ Matthias J Szabolcs,³ Sejal Morjaria,^{4,5} Sharon L Mount,² Natasha Rekhtman,¹ Elena Selbs,⁶ Zong-Mei Sheng,⁷ Yongli Xiao,⁷ David E Kleiner,⁸  Stefania Pittaluga,⁸  Jeffery K Taubenberger,⁷ Amy V Rapkiewicz⁶ & William D Travis¹ 

¹Department of Pathology, Memorial Sloan Kettering Cancer Center, New York, NY, ²Department of Laboratory Medicine and Pathology, University of Vermont Medical Center, Burlington, VT, ³Department of Pathology and Cell Biology, Columbia University, New York, ⁴Infectious Disease, Department of Medicine, Memorial Sloan Kettering Cancer Center, New York, ⁵Weill Cornell Medical College, New York, ⁶Department of Pathology, New York University Long Island School of Medicine, Mineola, NY, ⁷Viral Pathogenesis and Evolution Section, Laboratory of Infectious Diseases, National Institute of Allergy and Infectious Diseases, National Institutes of Health, and ⁸Center for Cancer Research, National Cancer Institute, National Institutes of Health, Bethesda, MD, USA

Date of submission 4 June 2020

Accepted for publication 27 June 2020

Published online Article Accepted 2 July 2020

Sauter J L, Baine M K, Butnor K J, Buonocore D J, Chang J C, Jungbluth A A, Szabolcs M J, Morjaria S, Mount S L, Rekhtman N, Selbs E, Sheng Z-M, Xiao Y, Kleiner D E, Pittaluga S, Taubenberger J K, Rapkiewicz A V & Travis W D.

(2020) *Histopathology* 77, 915–925. <https://doi.org/10.1111/his.14201>

Insights into pathogenesis of fatal COVID-19 pneumonia from histopathology with immunohistochemical and viral RNA studies

Introduction: We describe post-mortem pulmonary histopathologic findings of COVID-19 pneumonia in patients with a spectrum of disease course, from rapid demise to prolonged hospitalisation.

Methods and results: Histopathologic findings in post-mortem lung tissue from eight patients who died from COVID-19 pneumonia were reviewed. Immunohistochemistry (IHC) and next-generation sequencing (NGS) were performed to detect virus. Diffuse alveolar damage (DAD) was seen in all cases with a spectrum of acute phase and/or organising phase. IHC with monoclonal antibodies against SARS-CoV-2 viral nucleoprotein and spike protein detected virus in areas of acute but not organising DAD, with intracellular viral antigen and RNA expression seen predominantly in patients with duration of illness less than 10 days. Major vascular findings included thrombi in

medium- and large-calibre vessels, platelet microthrombi detected by CD61 IHC and fibrin microthrombi.

Conclusions: Presence of SARS-CoV-2 viral RNA by NGS early in the disease course and expression of viral antigen by IHC exclusively in the acute, but not in the organising phase of DAD, suggests that the virus may play a major role in initiating the acute lung injury of DAD, but when DAD progresses to the organising phase the virus may have been cleared from the lung by the patient's immune response. These findings suggest the possibility of a major change during the disease course of COVID-19 pneumonia that may have therapeutic implications. Frequent thrombi and microthrombi may also present potential targets for therapeutic intervention.

Address for correspondence: W D Travis, Department of Pathology, A525, Memorial Sloan Kettering Cancer Center, 1275 York Avenue, New York, NY 10065, USA. e-mail: travisw@mskcc.org

*These authors contributed equally to this study.

Keywords: COVID-19, diffuse alveolar damage, immunohistochemistry, lung histopathology, next-generation sequencing, SARS-CoV-2, thrombi, viral pneumonia

Introduction

In March of 2020, New York became the epicentre of the worldwide Coronavirus Disease 2019 (COVID-19) pandemic caused by severe acute respiratory syndrome coronavirus 2 (SARS-CoV-2), a novel coronavirus that emerged via animal to human transmission in Wuhan, China in late 2019.¹ As of 23 June 2020, there have been 8 993 659 reported COVID-19 cases and 469 587 COVID-19-related deaths globally.² Of these, 2 302 288 and 120 333 occurred in the United States, respectively, with New York State representing a large proportion, with 389 666 total cases and 24 782 deaths.^{3,4}

While most individuals exposed to SARS-CoV-2 remain asymptomatic or develop mild to moderate symptoms, including cough, fatigue and fever or chills, approximately 20% develop severe shortness of breath and respiratory failure resulting in acute respiratory distress syndrome requiring assisted oxygenation.⁵ Mortality in critically ill patients is high, with reports of 21–28% in hospitalised patients and 61% in critically ill patients.^{6–8} In New York specifically, mortality among COVID-19 patients requiring mechanical ventilation has been reported to reach up to 88%.⁹

Diffuse alveolar damage (DAD) has been the main finding in the emerging histopathologic studies of COVID-19 pneumonia,^{10–17} but there has been little attention focused on the progression of DAD from acute to organising phase and its relationship to clearance of SARS-CoV-2 from the lungs.

Herein, we report comprehensive post-mortem pulmonary histopathologic findings of COVID-19 pneumonia, throughout a spectrum of disease course, including immunohistochemistry (IHC) and viral RNA studies, to address key questions regarding the pathogenesis of this disease.

Materials and methods

STUDY DESIGN AND PATIENT COHORT

This study was conducted following expedited institutional review board approval (Protocol no. 17-630) and comprised review of lung pathology specimens from eight patients who died from COVID-19

pneumonia. Mean time interval from death to post-mortem examination was 53 h (range = 4–216). Lung tissue was fixed in formalin for at least 72 h. Haematoxylin and eosin (H&E)-stained sections were prepared. Histological examination was performed with all available lung tissue (median = 12.5 H&E slides; range = 7–20 sections, including at least one section from each lung lobe, per case). Antemortem diagnosis of COVID-19 was confirmed in all patients by real-time reverse transcriptase polymerase chain reaction (RT-PCR) (GeneExpert by Cepheid or Cobas SARS-CoV-2 by Roche Molecular Systems, Inc.).^{18,19} Five DAD cases from pre-COVID-19 era of various aetiologies served as control tissue for ancillary studies.

Patient demographics and clinical, laboratory and imaging data were extracted from medical records. These data and complete full autopsy findings from patients 1–5, 7 and 8 have also been reported separately in a clinical journal without emphasis on pulmonary histology.²⁰

HISTOLOGIC EVALUATION

Published criteria were used for classifying DAD as acute or organising phases.^{21,22} Details of histologic evaluation are summarised in Data S1.

IMMUNOHISTOCHEMISTRY

IHC was performed using two monoclonal antibodies to SARS-CoV comprising clone 001, (1:5 K; Sino Biological, Wayne, PA, USA) to viral nucleoprotein and clone 1A9 (1:1 K; GeneTex, Irvine, CA, USA) to the S2 spike protein. Both reagents were extensively analysed for their reactivity and specificity²³ and utilised on two to three tissue sections from each COVID-19 case and one to two sections from each control non-COVID DAD case. Methods of IHC for lymphoid markers and CD61 are summarised in Data S1.

VIRAL RNA DETECTION

RNA was extracted from the formalin-fixed paraffin-embedded (FFPE) autopsy sections and next-generation sequencing (NGS) was performed to detect virus, as previously described.²⁴ More information concerning the methods is in Data S1.

Results

PATIENT DEMOGRAPHICS, SOCIAL HISTORY AND COMORBIDITIES

All eight patients (four women, four men) were relatively young, with a median age of 57.5 years (range = 39–65). Most patients, 75% (six of eight), were obese. Median body mass index of the cohort was 33.9 kg/m² (range = 23.0–53.2). Five (62.5%) patients were never smokers, two (25%) were former smokers and one (patient 2) was a current smoker.

All patients, except patient 7, had multiple comorbidities. Most had either pre-diabetes or type II diabetes mellitus ($n = 5$), hyperlipidaemia ($n = 4$) and cardiovascular disease [either hypertension ($n = 6$) or prior history of myocardial infarction ($n = 1$)]. Patient 2 had chronic obstructive pulmonary disease, and patient 4 had obstructive sleep apnoea managed with home continuous positive airway pressure. The remaining patients had no documented pulmonary disease.

CLINICAL PRESENTATION

All patients presented in respiratory distress except patient 2, who became asystolic during ambulance transport and was pronounced dead shortly after arriving at the hospital. Duration of symptoms prior to hospital admission varied from a few days (patient 2) to up to 2 weeks (patients 7 and 8). All patients experienced shortness of breath and cough prior to admission. Fevers (100.7–102.9°F) were reported for all patients, except patients 2 and 8. Additional clinical features as well as laboratory findings are provided in Data S1.

RADIOGRAPHIC FINDINGS

Chest X-ray reports were available for seven patients, but not patient 2, as she died upon arrival at the hospital. Bilateral pulmonary infiltrates/opacities, suggestive of multifocal pneumonia, were seen in all seven patients.

MEDICAL MANAGEMENT AND HOSPITAL COURSE

Duration of disease from onset of symptoms to death ranged from 3 (patient 1) to 25 (patient 7) days (Table 1). All patients, except patients 1 and 2, were managed with mechanical ventilation (median duration = 2.5 days; range = < 1–11 days) (Table 1).

POST-MORTEM GROSS FINDINGS

Internal examinations revealed that the lungs were heavy in all cases, with combined post-mortem lung weights ranging from 1630 g (patient 3) to 2380 g (patient 6).

POST-MORTEM PATHOLOGIC FINDINGS

Major findings

The major findings in this study include (i) DAD with presence of viral antigen and RNA in acute DAD with duration of illness less than 10 days in contrast to loss of viral antigen and RNA in cases with more organising DAD with longer duration of illness, (ii) vascular thrombi including microthrombi, (iii) inflammatory cells differed between acute versus organising DAD with neutrophils in the former and chronic inflammatory cells in the latter, (iv) histologic findings of acute bronchopneumonia and (v) bronchitis and bronchiolitis (Table 1).

Major histological findings

Diffuse alveolar damage and other interstitial findings. Histological sections of lung in all cases showed heterogeneous features with varying stages of acute and/or organising DAD (Figure 1), sometimes adjacent to areas of relatively preserved alveolar parenchyma. The acute/exudative phase of DAD was the primary finding in cases 1 and 2, characterised by hyaline membranes, alveolar and interstitial oedema, with atypical type II pneumocyte proliferation, alveolar fibrin and frequent pneumocyte desquamation into alveolar spaces (Figure 1A–D). The latter may be a post-mortem artefact rather than a true pathological finding. Organising DAD, with or without focal acute changes, was the primary finding in the remaining cases. No acute DAD was seen in case 6. Organising DAD was characterised by alveolar wall thickening due to fibroblastic proliferation and prominent type II pneumocyte proliferation often with atypical reactive changes (Figure 1E). Pulmonary oedema was observed in seven cases (Figure 1B), with interlobular septal thickening by oedema seen in cases 1 and 4 (Figure 1A).

In areas showing acute phase of DAD, interstitial neutrophilic infiltrates were focally prominent (Figure 1C). In five of the six cases with organising DAD, there was mild to moderate interstitial chronic inflammation composed of lymphocytes, plasma cells and histiocytes in alveolar walls and within areas of

Table 1. Disease course and histopathologic findings in autopsy lung tissue from patients who died from COVID-19 pneumonia

Patient	Duration from onset of symptoms (days) [§]	Mechanical ventilation (duration in days) [§]	Attempted resuscitation	Phase of DAD	Interstitial inflammation [†]	Airway changes	Vascular changes [‡]	Infarct present
1	7	No	Yes	Acute	Neutrophils (ADAD)	Marked acute bronchitis and bronchiolitis; aspiration pneumonia	Acute vascular inflammation in areas of acute pneumonia; focal chronic venular inflammation; platelet microthrombi	No
2	3	No	Yes	Acute	Neutrophils (ADAD)	Mild acute bronchitis and bronchiolitis	Platelet microthrombi	No
3	9	Yes (2)	Yes	Acute and organising	Lymphocytes (ODAD) and neutrophils (ADAD)	Mild acute bronchitis and bronchiolitis; mild focal chronic bronchiolitis	Medium sized arterial thrombi; fibrin and platelet microthrombi; mild chronic venular inflammation	No
4	16	Yes (1)	No	Acute and organising	Lymphocytes (ODAD) and neutrophils (ADAD)	Mild acute bronchitis and bronchiolitis; mild focal chronic bronchiolitis	Platelet microthrombi	No
5	13	Yes (4)	Yes	Organising and acute (focal)	Lymphocytes (ODAD) and neutrophils (ADAD)	Mild acute bronchitis and bronchiolitis	Medium sized arterial thrombi; platelet microthrombi; mild chronic venular inflammation	Yes
6	20	Yes (11)*	No	Organising	Lymphocytes (ODAD) and eosinophils	Mild chronic bronchitis and bronchiolitis	Large arterial thrombus; Platelet microthrombi	No
7	25	Yes (9)	No	Organising and acute (focal)	Lymphocytes (ODAD) and neutrophils (ADAD)	Mild acute and chronic bronchitis and bronchiolitis	Acute vascular inflammation in areas of acute pneumonia; platelet microthrombi	No
8	17	Yes (<1)	No	Organising and acute (focal)	Lymphocytes (ODAD) and neutrophils (ADAD)	Mild acute and chronic bronchiolitis; mucus plugging in proximal bronchi	Large and medium sized arterial thrombi; fibrin and platelet microthrombi; mild chronic venular inflammation	No

ADAD, Acute phase of DAD; DAD, Diffuse alveolar damage; ODAD, Organising phase of DAD.

*Patient was intubated twice, initially for 10 days, then off for 4 days before reintubating for 1 day.

[†]The neutrophils were seen focally in areas of acute DAD and the lymphocytes in areas of organising DAD.

[‡]Vascular changes seen on histological examination of haematoxylin and eosin (H&E)-stained slides without assistance of immunohistochemistry include thrombi, fibrin microthrombi and vasculitis. Platelet microthrombi by CD61 immunohistochemistry were seen in all cases.

[§]Clinical and limited pulmonary pathology data for patients 1–5, 7 and 8 are published separately.²⁰

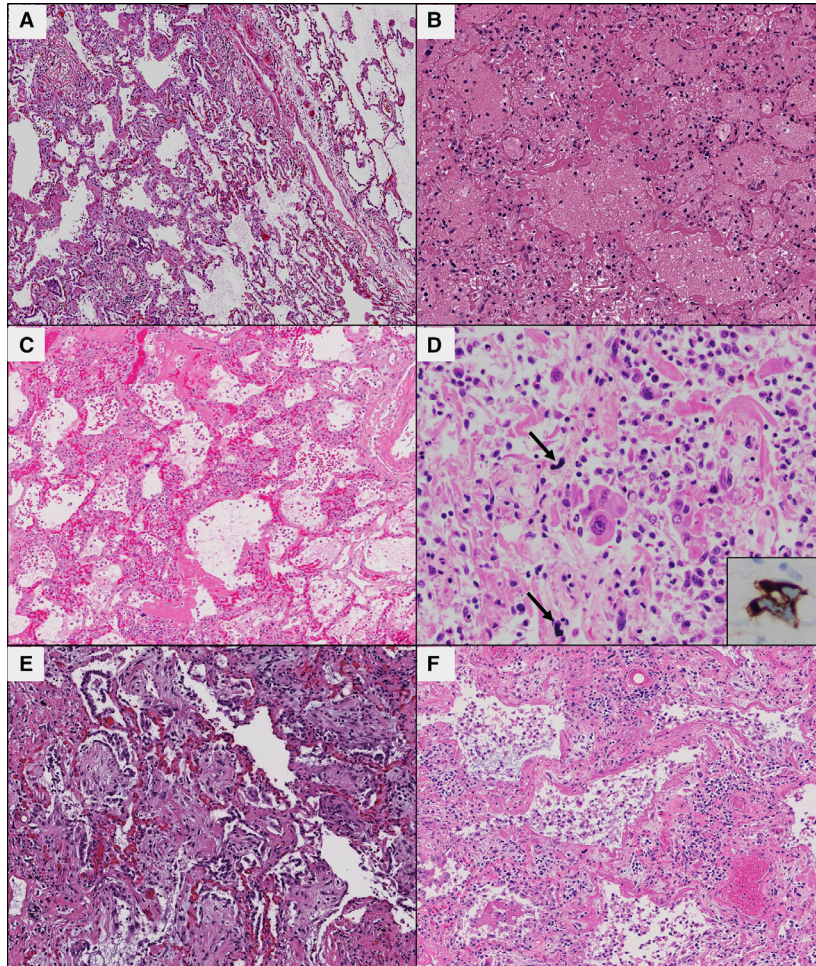


Figure 1. Spectrum of diffuse alveolar damage (DAD) seen in COVID-19 pneumonia. **A**, All cases demonstrated DAD, seven of eight of which showed a component of acute phase DAD. Note the demarcation between affected lung parenchyma with thickened alveolar septa and hyaline membranes (lower left) and the relatively preserved lung parenchyma (upper right) separated by a thickened oedematous interlobular septum. **B**, Oedema of variable severity was seen in all cases and is marked in this example. Note also the conspicuous hyaline membranes. **C**, The presence of interstitial neutrophilic infiltrates was focally seen in areas with acute DAD. **D**, Reactive type II pneumocytes within alveolar spaces showed abundant eosinophilic cytoplasm, irregular nuclear contours, occasional binucleation, vesicular condensed chromatin and prominent macronucleoli. Intracapillary megakaryocytes (arrows) were also present within alveolar capillaries and were highlighted by CD61 immunohistochemistry (inset). **E**, Lungs from six patients showed organising phase DAD alone or in combination with acute phase DAD, with characteristic type II pneumocyte and fibroblastic proliferation within alveolar walls and focal intraluminal plugs of loose connective tissue. **F**, Some areas within organising DAD showed interstitial chronic inflammation.

proliferating connective tissue (Figure 1E), most prominent in case 6 (Figure 1F).

Reactive type II pneumocytes displayed abundant eosinophilic cytoplasm with focal areas of cytoplasm showing a foamy appearance. Nuclei were enlarged, many with irregular nuclear contours, containing vesicular condensed chromatin and prominent macronucleoli (Figure 1D). No viral inclusions were seen.

Details of inflammatory cell infiltrates, bronchial and bronchiolar lesions (Figure S1), acute

bronchopneumonia, vascular lesions including thrombi and vascular inflammation (Figure S2) as well as minor histological findings are included in Data S1.

IMMUNOHISTOCHEMISTRY

IHC with a monoclonal antibody against SARS-CoV nucleoprotein detected virus in six of eight (75%) study cases (Table 2) and was negative in all non-

Table 2. Viral detection by next-generation sequencing and immunohistochemistry and corresponding histology

Case	Onset to death (days)	Viral RNA*	Anti-SARS-CoV spike protein (clone 1A9)		Anti-SARS-CoV nucleoprotein (clone 001)		Histologic findings in FFPE tissue used for NGS
			Acute DAD	Organising DAD	Acute DAD	Organising DAD	
1	7	Detected	++	NA	++	NA	Acute DAD
2	3	Detected	++	NA	++	NA	Acute DAD
3	9	Detected	+	–	+	–	Acute and organising DAD
4	16	Not detected	+‡	NA	+	NA	Predominantly organising DAD with focal acute DAD
5	13	Not detected	+‡	NA	+	NA	Predominantly organising DAD with focal acute DAD
6	20	Not detected	NA	–	NA	–	Organising DAD
7	25	Not detected	NA†	NA†	NA†	NA†	Necrotising pneumonia
8	17	Not detected	+‡	–	+	–	Organising DAD with very focal acute DAD

DAD, Diffuse alveolar damage; NA, Not applicable; ++, Strong positive; +, Positive; –, Negative; FFPE, Formalin-fixed paraffin-embedded; NGS, Next-generation sequencing.

*The range of the total reads generated from these samples is 94 185 253 to 190 608 325. The range of viral reads in positive cases is 1497–145 854. The range of viral reads in negative cases is 4–177. A threshold for detection was defined as a minimum of 1000 reads mapped to the SARS-CoV-2 genome.

†The section available for immunohistochemistry was entirely composed of an area of acute necrotising pneumonia without features of DAD.

‡Viral antigen detected in at least one section.

COVID DAD control tissue, confirming previously established antibody specificity.²³ Similar results were obtained with monoclonal antibody against SARS-CoV spike protein, but staining was weaker. Most notably, staining for both antibodies was confined to areas of acute DAD but absent in areas with organising phase of DAD, clearly highlighted in case 3, with both phases of DAD represented in a single section (Figure 2A,B). This finding also accounts for lack of immunoreactivity in two cases (6 and 7) due to the absence of acute DAD in the sections available for staining. Viral antigen was detected in hyaline membranes in all positive cases, but diffuse intracellular staining in the cytoplasm of regenerating and reactive type II pneumocytes and in alveolar macrophages (Figure 2C,D) was seen only in two patients with the shortest disease course (cases 1 and 2). In only one of these cases (case 1), weak cytoplasmic staining was also seen in endothelial cells of scattered venules and alveolar capillaries (Figure 2E). Of note, this case (case 1) demonstrated the highest amount of viral antigen by IHC on representative sections compared to all other cases in the cohort. Interestingly, viral antigen was detected in bronchial epithelial cells only in case 2 (shortest disease course and very high viral load) and only with the antibody against

nucleoprotein. Similarly, very rare reactive pneumocytes and alveolar macrophages stained with the antibody against nucleoprotein but not against S2 spike subunit in cases with longer disease course (cases 5 and 8; disease duration 16 and 17 days, respectively).

Results of IHC for lymphoid markers and CD61 are summarised in Data S1.

VIRAL RNA DETECTION

In cases 1–3 with time from disease onset to death of less than 10 days (7, 3 and 9 days, respectively) and predominantly acute DAD histologically, SARS-CoV-2 viral RNA was detected by NGS,^{25,26} but it was not detected in cases 4–8 where duration of disease was greater than 10 days (16, 13, 20, 25 and 17 days, respectively) and lung histology showed predominantly organising DAD (Table 2). Notably, these cases were either negative for viral antigen by IHC (cases 6 and 7) or positive staining was seen predominantly in hyaline membranes within focal areas of acute DAD (cases 4, 5 and 8). Case 3 was an exception, in that viral RNA was detected at a low level by NGS despite staining by IHC being confined to hyaline membranes. Of note in this case, the block used for

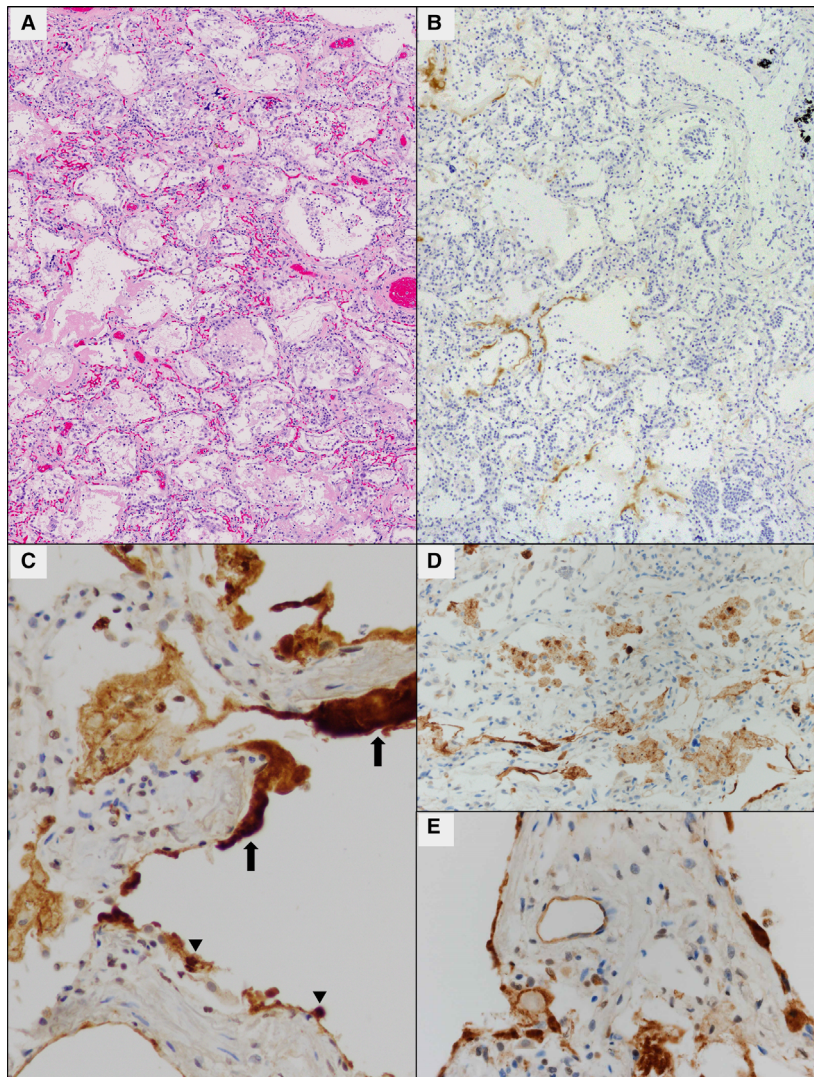


Figure 2. Viral antigen detection by immunohistochemistry (IHC) against SARS-CoV nucleoprotein [monoclonal antibody (mAb) 001]. A, In this example (case 3) both acute and organising phases of DAD are present in a single section. Areas with organising DAD (upper right) that lack hyaline membranes failed to demonstrate the presence of viral antigen by IHC, while areas with acute DAD (lower left) showed staining in hyaline membranes but not in pneumocytes (B). C, In all IHC-positive cases, viral antigen was detected in hyaline membranes (thick arrows) within areas of acute phase DAD, and in two cases diffusely within regenerating and reactive type II pneumocytes (arrowheads). Viral antigen was also present in alveolar macrophages in these latter two cases (D). In case 1, the case with the most viral antigen detected by IHC, weak cytoplasmic staining was observed in endothelial cells of scattered venules and alveolar capillaries (E).

RNA extraction contained more abundant areas of acute DAD than the section used for IHC, which may explain this result.

Discussion

Our study provides novel observations documenting a major change that occurs in the pathogenesis of COVID-19 pneumonia as DAD progresses from the

acute to the chronic phase. The presence of SARS-CoV antigen by IHC exclusively in areas of acute phase DAD but not in areas of organising phase of DAD and detection of viral RNA by NGS early in the course of disease (<10 days) suggest that the virus plays a major role in initiating acute lung injury of DAD. However, after the first 10 days of illness and/or when DAD progresses to the organising phase, the viral RNA and protein may have been cleared by the patient's immune response. While this manuscript

was in review, another study was published validating our findings that SARS-CoV-2 is mainly present in early stages of DAD and was absent in areas of organising phase of DAD.²⁷ In contrast to our report, this study used a single polyclonal rather than two monoclonal antibodies for IHC and did not report any staining of control non-COVID DAD cases or provide viral RNA testing of lung tissues.²⁷

Our finding, that both monoclonal antibodies showed IHC expression of viral antigen in type II pneumocytes and alveolar macrophages as well as hyaline membranes, corresponds well with the localisation of coronavirus virions previously identified by electron microscopy.²⁸ The nucleoprotein antibody (001) showed more extensive staining than the spike protein antibody (1A9), raising consideration of differences in sensitivity and specificity among antibodies. We noted peculiar staining of hyaline membranes with both SARS-CoV antibodies in all IHC-positive cases. Although non-specific staining would be a consideration, the absence of staining in hyaline membranes of control non-COVID DAD cases confirms its specificity. Another report of identification of virions in hyaline membranes supports our finding.²⁸ This observation of the presence of viral protein antigens in hyaline membranes in the absence of detectable viral RNA is not unique to SARS-CoV-2 infections, and has also been observed in influenza A autopsy studies from the 1918 and 2009 pandemics.^{24,29} Viral proteins still detectable in hyaline membrane material probably reflect remnants of lytic infections. RNA is much less stable than proteins given ubiquitous RNAases and this is the probable explanation for our observations and those in prior influenza autopsy studies.³⁰

Notably, in our cohort, the most prominent intracellular viral antigen was detected in the two cases (cases 1 and 2) with the most acute presentation and rapid disease course (7 and 3 days, respectively) and with only acute DAD histology, and corresponds to the cases with highest levels of SARS-CoV-2 RNA detected by NGS in this cohort. This pattern of expression in both pneumocytes and hyaline membranes during the initial injury, and apparent progressive loss of expression from pneumocytes later in the disease course, may represent the process of viral clearance, whereby viral proteins are released into alveolar spaces from infected pneumocytes damaged by direct lytic action and/or by inflammatory cell/immune mediated injury, and are cleared by the patient's immune system later in the disease course, histologically manifesting as organising phase of DAD as the lung attempts to repair. Also, it is important to note that the histological findings are

heterogeneous in these cases, with varying amounts of acute and organising DAD in different areas of the same lungs. Therefore, it is possible that clearance of the virus may be a local rather than global effect, until the DAD progresses to exclusively organising phase.

As published data rapidly accumulate regarding SARS-CoV IHC in lung tissues from patients with COVID-19 pneumonia, careful attention to methodology must be observed, including particular antibodies (polyclonal versus monoclonal) and antigen detected (spike versus nucleoprotein), pattern of lung injury evaluated (acute versus organising DAD or bronchopneumonia), localisation of immunoreactivity (pneumocytes, hyaline membranes, macrophages, endothelial cells or bronchial epithelial cells) and duration of illness. Variation in each of these factors may result in differences in reported results.^{27,28,31–33} It should also be noted that some antibodies being utilised in published reports, including those we utilised, are not specific to SARS-CoV-2, because they also react with SARS-CoV-1. However, in the current pandemic, the differential diagnosis between these two SARS-CoV infections is not a major question. In addition, although we confirmed the presence of viral antigen in lung tissue from our COVID-19 patients, we did not identify any definite viral inclusions (Supporting information, Results and Discussion).

Interestingly, lung histology from two patients who died rapidly with little or no mechanical ventilation showed acute DAD, while lung histology from the other six patients who received mechanical ventilation showed predominantly organising DAD, in addition to acute changes in five patients. Additionally, the type of inflammation in the lung changed with the phase of DAD from neutrophils in the acute phase to chronic inflammatory interstitial infiltrates in organising DAD. This finding raises the consideration that lymphocytes, plasma cells and histiocytes may also have a pathogenic role, perhaps in the immune response to and clearance of the virus. We cannot exclude the possibility that the presence of these chronic inflammatory cells could be related to the longer periods of mechanical ventilation in these patients. However, in DAD due to other aetiologies, neutrophils have been described early in the course of disease and other chronic inflammatory cells in later stages regardless of whether mechanical ventilation has been used or not.^{21,34–39} In other viral pneumonias, including influenza^{40–43} and Ebola,⁴⁴ the host inflammatory response has been shown to play a distinct role in pathogenesis in addition to direct damage from viral infections. It is reasonable to hypothesise that this is also the case in severe

SARS-CoV-2 infections, but more research on this question is needed.

Emerging literature regarding COVID-19 pneumonia supports our findings that viral clearance from the lung may occur as DAD progresses to the organising phase. Clinical evidence has shown that SARS-CoV-2 viral load, transmissibility and pharyngeal virus shedding peaks within the first week of disease.^{45–48} In a pathology study, Menter *et al.* did not find viral RNA by RT–quantitative PCR (RT–qPCR) in lung tissue in one of 21 post-mortem cases, but correlation with the histological phase of DAD was not mentioned.⁴⁹ Adachi *et al.* briefly noted, without mention of its significance, detection of SARS-CoV-2 antigen by IHC in pneumocytes of earlier DAD rather than ‘progressed’ lesions, which may represent organising DAD.³¹ Martines *et al.* did not detect SARS-CoV antigen by IHC in lung tissue of one case with predominantly organising DAD by histology, but six of seven cases that showed acute DAD and/or acute bronchopneumonia were viral antigen-positive.²⁸ Mild IHC positivity was found in one case with only mild organising DAD. Unfortunately, this study did not correlate the IHC positivity with specific histological features such as areas of acute versus organising DAD or bronchopneumonia.²⁸ Our findings in COVID-19 pneumonia are similar to those observed by Shieh *et al.* in H1N1 influenza viral pneumonia, where influenza A viral RNA by RT–PCR and antigen by IHC were detected less frequently in lungs of patients with longer duration of illness (i.e. greater than 10 days) compared to patients with a shorter disease course.⁵⁰ The phenomenon of viral clearance from the respiratory tract in SARS-CoV2 pneumonia was also noted in a recent case report.⁵¹ However, neither Shieh nor Shao *et al.* correlated these findings with histological patterns of DAD. The distinct change in histology from acute DAD pattern when the virus is present in lung tissue, to the organising phase of DAD along with the presence of chronic inflammatory infiltrates when the virus has been cleared from lung tissue, suggests a fundamental transition in the pathogenesis of COVID-19 pneumonia depending on the stage of DAD and/or duration of illness. This is an interesting observation and should be further studied in other viral pneumonias to determine if it is unique to COVID-19 pneumonia. These findings may have important therapeutic implications, such that antiviral agents may be useful in early stages of COVID-19 pneumonia, but after 10–14 days, when virus has been cleared from the lungs, it may be best to transition the focus of therapy to managing organising DAD. However, determining the

clinical utility of our findings for guiding therapy requires validation in larger cohorts.

Viral antigen was detected by IHC very focally in endothelial cells in one case in this cohort. However, this is insufficient evidence to suggest primary infection of endothelial cells plays a major role in vascular injury or DAD in COVID-19 pneumonia. The suggestion based upon ultrastructural findings, that SARS-CoV-2 directly infects endothelial cells,^{52,53} has been disputed. Goldsmith *et al.* pointed out that images published as putative virions within endothelial cells actually represented normal cellular structures such as endoplasmic reticulum rather than virus.⁵⁴ As in our study, Shieh *et al.* described positive IHC for H1N1 influenza in endothelium only in rare cases.⁵⁰ Furthermore, although we did observe thrombi, microthrombi and focal vascular inflammation (Supporting information, Discussion and Supporting information, Figure S2) we did not observe lesions of thrombotic necrotising capillary injury, endothelial cell necrosis or endothelialitis as reported by others.^{32,52} Nevertheless, further study of the role of SARS-CoV-2 in endothelial cell injury is warranted to more clearly understand the pathogenesis of viral infection in this disease.

In summary, our findings suggest that the initial lung injury in fatal COVID-19 pneumonia is directly caused by SARS-CoV-2 in the acute phase of DAD. As DAD progresses to the organising phase viral RNA and antigen become undetectable, suggesting possible clearance by the patient’s immune response. These findings suggest the pathogenesis of COVID-19 pneumonia undergoes a major change during disease course and raises consideration for different therapeutic approaches, depending on whether DAD has progressed to the organising phase.

Acknowledgements

This work was supported in part by the Intramural Research Program of the National Institutes of Health and National Institute of Allergy and Infectious Diseases (J.K.T.).

Conflicts of interest

The authors have no conflicts of interest to disclose.

Author contributions

The study was designed by W. Travis, J. Sauter and M. Baine. The manuscript was written by J. Sauter, B.

Baine, and W. Travis, and partially by A. Jungbluth, M. Szabolcs, J. Taubenberger and A. Rapkiewicz. Autopsies were performed by A. Rapkiewicz and S. Mount. Histology was performed by J. Sauter, M. Baine, K. Butnor, S. Mount, N. Rekhman, E. Selbs, A. Rapkiewicz and W. Travis. Molecular analysis was performed by J. Taubenberger, Z-M Sheng and Y. Xiao. A. Jungbluth and M. Szabolcs developed and performed immunohistochemistry assays. S Morjaria analyzed clinical data. All authors read and approved the manuscript.

References

- World Health Organisation (WHO). Pneumonia of unknown cause – China [internet]. 2020. Updated 25 May 2020. Available at: <http://www.who.int/csr/don/05-january-2020-pneumonia-of-unknown-cause-china/en/>
- World Health Organisation (WHO). Coronavirus disease (COVID-19): Situation Report – 155 [internet]. 2020. Updated 24 June 2020. Available at: [https://www.who.int/docs/default-source/coronaviruse/situation-reports/20200523-covid-19-sitrep-155.pdf?sfvrsn=9626d639_2](https://www.who.int/docs/default-source/coronaviruse/situation-reports/20200523-covid-19-sitrep-155-20200523-covid-19-sitrep-155.pdf?sfvrsn=9626d639_2)
- Centers for Disease Control (CDC). Coronavirus Disease 2019 (COVID-19): Cases, Data and Surveillance [internet]. 2020. Updated 24 June 2020. Available at: <https://www.cdc.gov/coronavirus/2019-ncov/cases-updates/cases-in-us.html>
- New York State Department of Health. Workbook: NYS-COVID-19-Tracker [internet]. 2020. Updated 24 June 2020. Available at: <https://covid19tracker.health.ny.gov/views/NYS-COVID19-Tracker/NYSDOHCOVID-19Tracker-Fatalities?%3Aembed=yes&%3Atoolbar=no&%3Atabs=en>
- Zhu J, Ji P, Pang J et al. Clinical characteristics of 3,062 COVID-19 patients: a meta-analysis. *J. Med. Virol.* 2020; **92**: 1902–1914.
- Wu C, Chen X, Cai Y et al. Risk factors associated with acute respiratory distress syndrome and death in patients with coronavirus disease 2019 pneumonia in Wuhan, China. *JAMA Intern. Med.* 2020; **180**: 1–11.
- Yang X, Yu Y, Xu J et al. Clinical course and outcomes of critically ill patients with SARS-CoV-2 pneumonia in Wuhan, China: a single-centered, retrospective, observational study. *Lancet Respir. Med.* 2020; **8**: 475–481.
- Zhou F, Yu T, Du R et al. Clinical course and risk factors for mortality of adult inpatients with COVID-19 in Wuhan, China: a retrospective cohort study. *Lancet* 2020; **28**: 1054–1062.
- Richardson S, Hirsch JS, Narasimhan M et al. Presenting characteristics, comorbidities, and outcomes among 5700 patients hospitalized with COVID-19 in the New York City area. *JAMA* 2020; **323**: 2052–2059.
- Barnes BJ, Adrover JM, Baxter-Stoltzfus A et al. Targeting potential drivers of COVID-19: neutrophil extracellular traps. *J. Exp. Med.* 2020; **1**: 217.
- Barton LM, Duval EJ, Stroberg E, Ghosh S, Mukhopadhyay S. COVID-19 autopsies, Oklahoma, USA. *Am. J. Clin. Pathol.* 2020; **153**: 725–733.
- Lax SF, Skok K, Zechner P et al. Pulmonary arterial thrombosis in COVID-19 with fatal outcome: results from a prospective, single-center, clinicopathologic case series. *Ann. Intern. Med.* 2020; **173**: 350–361.
- Tian S, Xiong Y, Liu H et al. Pathological study of the 2019 novel coronavirus disease (COVID-19) through postmortem core biopsies. *Mod. Pathol.* 2020; **33**: 1007–1014.
- Wichmann D, Sperhake JP, Lutgehetmann M et al. Autopsy findings and venous thromboembolism in patients with COVID-19. *Ann. Intern. Med.* 2020; **173**: 268–277.
- Xu Z, Shi L, Wang Y et al. Pathological findings of COVID-19 associated with acute respiratory distress syndrome. *Lancet Respir. Med.* 2020; **8**: 420–422.
- Yan L, Mir M, Sanchez P et al. COVID-19 in a hispanic woman. *Arch. Pathol. Lab. Med.* 2020; **144**: 1041–1047.
- Fox SE, Akmatbekov A, Harbert JL, Li G, Brown JQ, Vander Heide RS. Pulmonary and cardiac pathology in African American patients with COVID-19: an autopsy series from New Orleans. *Lancet Respir. Med.* 2020; **8**: 681–686.
- Cepheid. Xpert Xpress SARS-CoV-2 Test. Cepheid; 2020. Updated 25 May 2020. Available at: https://www.cepheid.com/en_US/package-inserts/1615
- Roche Diagnostics. Cobas® SARS-CoV-2 Test (for the COVID-19 Coronavirus) [internet]. Roche Diagnostics. 2020. Updated 25 May 2020. Available at: <https://diagnostics.roche.com/us/en/products/params/cobas-sars-cov-2-test.html>
- Rapkiewicz A, Mai X, Carsons SE et al. Megakaryocytes and platelet-fibrin thrombi characterize multi-organ thrombosis at autopsy in COVID-19: a case series. *EClinicalMedicine.* 2020; **24**: 100434.
- Katzenstein AL, Bloor CM, Leibow AA. Diffuse alveolar damage – the role of oxygen, shock, and related factors. A review. *Am. J. Pathol.* 1976; **85**: 209–228.
- Travis W, Colby T, Koss M et al. Diffuse alveolar damage and acute interstitial pneumonia. In King D ed. *Nonneoplastic disorders of the lower respiratory tract*. Washington, DC: American Registry of Pathology, 2002: 89–106.
- Szabolcs M, Sauter JL, Geronimo JA et al. Identification of immunohistochemical reagents for in-situ protein expression analysis of coronavirus-associated changes in human tissues. *Appl. Immunohistochem. Mol. Morphol.* 2020. Epub ahead of print.
- Sheng ZM, Chertow DS, Ambroggio X et al. Autopsy series of 68 cases dying before and during the 1918 influenza pandemic peak. *Proc. Natl Acad. Sci. USA* 2011; **108**: 16416–16421.
- Xiao Y, Park JK, Williams S et al. Deep sequencing of 2009 influenza A/H1N1 virus isolated from volunteer human challenge study participants and natural infections. *Virology* 2019; **534**: 96–107.
- Xiao YL, Ren L, Zhang X et al. Deep sequencing of H7N9 influenza A viruses from 16 infected patients from 2013 to 2015 in Shanghai reveals genetic diversity and antigenic drift. *mSphere* 2018; **19**: 3.
- Schaefer IM, Padera RF, Solomon IH et al. In situ detection of SARS-CoV-2 in lungs and airways of patients with COVID-19. *Mod. Pathol.* 2020. Epub ahead of print.
- Martines RB, Ritter JM, Matkovic E et al. Pathology and pathogenesis of SARS-CoV-2 associated with fatal coronavirus disease, United States. *Emerg. Infect. Dis.* 2020; **21**: 26.
- Gill JR, Sheng ZM, Ely SF et al. Pulmonary pathologic findings of fatal 2009 pandemic influenza A/H1N1 viral infections. *Arch. Pathol. Lab. Med.* 2010; **134**: 235–243.
- Lu L, Li J, Moussaoui M, Boix E. Immune modulation by human secreted RNases at the extracellular space. *Front. Immunol.* 2018; **9**: 1012.
- Adachi T, Chong JM, Nakajima N et al. Clinicopathologic and immunohistochemical findings from autopsy of patients with COVID-19, Japan. *Emerg. Infect. Dis.* 2020; **15**: 26.

32. Magro C, Mulvey JJ, Berlin D *et al.* Complement associated microvascular injury and thrombosis in the pathogenesis of severe COVID-19 infection: a report of five cases. *Transl. Res.* 2020; **220**; 1–13.
33. Zhang H, Zhou P, Wei Y *et al.* Histopathologic changes and SARS-CoV-2 immunostaining in the lung of a patient with COVID-19. *Ann. Intern. Med.* 2020; **172**: 629–632.
34. Nakajima T, Suarez CJ, Lin KW *et al.* T cell pathways involving CTLA4 contribute to a model of acute lung injury. *J. Immunol.* 2010; **184**: 5835–5841.
35. Lee WL, Downey GP. Neutrophil activation and acute lung injury. *Curr. Opin. Crit. Care* 2001; **7**: 1–7.
36. Rinaldo JE, Christman JW. Mechanisms and mediators of the adult respiratory distress syndrome. *Clin. Chest Med.* 1990; **11**: 621–632.
37. Verjans E, Kanzler S, Ohl K *et al.* Initiation of LPS-induced pulmonary dysfunction and its recovery occur independent of T cells. *BMC Pulmon. Med.* 2018; **18**: 174.
38. Pratt PC. Pathology of adult respiratory distress syndrome. *Monogr. Pathol.* 1978; **19**: 43–57.
39. Tomaszewski JF Jr. Pulmonary pathology of acute respiratory distress syndrome. *Clin. Chest Med.* 2000; **21**: 435–466.
40. Kash JC, Walters KA, Davis AS *et al.* Lethal synergism of 2009 pandemic H1N1 influenza virus and *Streptococcus pneumoniae* coinfection is associated with loss of murine lung repair responses. *MBio* 2011; **2**: e00172–e00211.
41. Kash JC, Xiao Y, Davis AS *et al.* Treatment with the reactive oxygen species scavenger EUK-207 reduces lung damage and increases survival during 1918 influenza virus infection in mice. *Free Rad. Biol. Med.* 2014; **67**: 235–247.
42. Taubenberger JK, Morens DM. The pathology of influenza virus infections. *Annu. Rev. Pathol.* 2008; **3**: 499–522.
43. Taubenberger JK, Kash JC, Morens DM. The 1918 influenza pandemic: 100 years of questions answered and unanswered. *Sci. Transl. Med.* 2019; **24**: 502.
44. Kash JC, Walters KA, Kindrachuk J *et al.* Longitudinal peripheral blood transcriptional analysis of a patient with severe Ebola virus disease. *Sci. Transl. Med.* 2017; **12**: 385.
45. Bullard J, Dust K, Funk D *et al.* Predicting infectious SARS-CoV-2 from diagnostic samples. *Clin. Infect. Dis.* 2020. Epub ahead of print.
46. Cheng HY, Jian SW, Liu DP, Ng TC, Huang WT, Lin HH. Contact tracing assessment of COVID-19 transmission dynamics in Taiwan and risk at different exposure periods before and after symptom onset. *JAMA Intern. Med.* 2020; **180**: 1156–1163.
47. Huang JT, Ran RX, Lv ZH *et al.* Chronological changes of viral shedding in adult inpatients with COVID-19 in Wuhan, China. *Clin. Infect. Dis.* 2020. Epub ahead of print.
48. Wölfel R, Corman VM, Guggemos W *et al.* Virological assessment of hospitalized patients with COVID-2019. *Nature* 2020; **581**: 465–469.
49. Menter T, Haslbauer JD, Nienhold R *et al.* Post-mortem examination of COVID19 patients reveals diffuse alveolar damage with severe capillary congestion and variegated findings of lungs and other organs suggesting vascular dysfunction. *Histopathology* 2020; **77**: 198–209.
50. Shieh WJ, Blau DM, Denison AM *et al.* 2009 pandemic influenza A (H1N1): pathology and pathogenesis of 100 fatal cases in the United States. *Am. J. Pathol.* 2010; **177**: 166–175.
51. Shao C, Liu H, Meng L *et al.* Evolution of severe acute respiratory syndrome coronavirus 2 RNA test results in a patient with fatal coronavirus disease 2019: a case report. *Hum. Pathol.* 2020; **101**: 82–88.
52. Varga Z, Flammer AJ, Steiger P *et al.* Endothelial cell infection and endotheliitis in COVID-19. *Lancet* 2020; **395**: 1417–1418.
53. Su H, Yang M, Wan C *et al.* Renal histopathological analysis of 26 postmortem findings of patients with COVID-19 in China. *Kidney Int.* 2020; **98**: 219–227.
54. Goldsmith CS, Miller SE, Martines RB, Bullock HA, Zaki SR. Electron microscopy of SARS-CoV-2: a challenging task. *Lancet* 2020; **395**: e99.

Supporting Information

Additional Supporting Information may be found in the online version of this article:

Figure S1. Spectrum of airway injury in COVID-19 pneumonia.

Figure S2. Spectrum of vascular changes in COVID-19 pneumonia.

Data S1. Supplemental material.